The Astrophysical Journal, 694:L49–L53, 2009 March 20 doi:10.1088/0004-637X/694/1/L49

NUCLEOSYNTHESIS MODES IN THE HIGH-ENTROPY WIND OF TYPE II SUPERNOVAE: COMPARISON OF CALCULATIONS WITH HALO-STAR OBSERVATIONS

K. Farouqi[1,2], K.-L. Kratz[3], L. I. Mashonkina[4], B. Pfeiffer[2], J. J. Cowan[5], F.-K. Thielemann[6], and J. W. Truran[1,7]
[1] Department of Astrophysics and Astronomy, University of Chicago, Chicago, IL 60637, USA; farouqi@uchicago.edu, truran@nova.uchicago.edu
[2] Institut für Kernchemie, Universität Mainz, D-55128 Mainz, Germany; BPfeiffe@uni-mainz.de
[3] Max-Planck-Institut für Chemie (Otto-Hahn-Institut), D-55128 Mainz, Germany; klkratz@uni-mainz.de
[4] Institute of Astronomy, Russian Academy of Science, RU-119017 Moscow, Russia; lima@inasan.ru
[5] Homer L. Dodge Department of Physics and Astronomy, University of Oklahoma, Norman, OK 73019, USA; cowan@nhn.ou.edu
[6] Departement Physik, Universität Basel, CH-4056 Basel, Switzerland; F-K.Thielemann@unibas.ch
[7] Physics Division, Argonne National Laboratory, Argonne, IL 60439, USA; truran@nova.uchicago.edu
Received 2008 July 11; accepted 2009 January 12; published 2009 February 27

ABSTRACT

While the high-entropy wind (HEW) of Type II supernovae remains one of the more promising sites for the rapid neutron-capture (*r*-) process, hydrodynamic simulations have yet to reproduce the astrophysical conditions under which the latter occurs. We have performed large-scale network calculations within an extended parameter range of the HEW, seeking to identify or to constrain the necessary conditions for a full reproduction of all *r*-process residuals $N_{r,\odot} = N_\odot - N_{s,\odot}$ by comparing the results with recent astronomical observations. A superposition of weighted entropy trajectories results in an excellent reproduction of the overall $N_{r,\odot}$ pattern beyond Sn. For the lighter elements, from the Fe group via Sr–Y–Zr to Ag, our HEW calculations indicate a transition from the need for clearly different sources (conditions/sites) to a possible co-production with *r*-process elements, provided a range of entropies are contributing. This explains recent halo-star observations of a clear noncorrelation of Zn and Ge and a weak correlation of Sr–Zr with heavier *r*-process elements. Moreover, new observational data on Ru and Pd also seem to confirm a partial correlation with Sr as well as the main *r*-process elements (e.g., Eu).

Key words: nuclear reactions, nucleosynthesis, abundances – stars: abundances – stars: Population II

1. INTRODUCTION

A rapid neutron-capture process (*r*-process) is traditionally believed to be responsible for the synthesis of about half of the heavy elements above Fe (Burbidge et al. 1957; Cameron 1957). The astrophysical site in which this mechanism operates is, however, still uncertain. For this reason, a model-independent approach, i.e. the classical "waiting-point" approximation, has been utilized for many years (see, e.g., Cowan et al. 1991; Kratz et al. 1993, 2007a). This simple model has helped to gain increased insight into the systematics of the *r* process: e.g., its dependence on nuclear-physics input and its sensitivity to astrophysical conditions (see, e.g., Pfeiffer et al. 2001; Kratz et al. 2007b). In realistic explosive scenarios, the necessary conditions for high neutron-to-seed ratios ($Y_n/Y_{\rm seed}$) can only be obtained in very neutron-rich low-entropy (S) environments, related, e.g., to neutron-star ejecta from neutron-star mergers (NSMs), or in moderately neutron-rich high-S scenarios, such as the high-entropy wind (HEW) of core-collapse Type II supernovae (SNe II). As observations of heavy-element abundance patterns in metal-poor stars in the early Galaxy (see, e.g., Sneden & Cowan 2003; Cowan & Sneden 2006) and Galactic chemical-evolution considerations both seem to disfavor NSM (Argast et al. 2004), we will focus here on the HEW scenario. Moreover, since even the most recent hydrodynamical simulations encounter problems in the time evolution of the HEW bubble and/or in the attainment of sufficiently high entropies, we continue to use parameterized dynamic network calculations to explore the dependence on nuclear properties and highlight a detailed understanding of the HEW nucleosynthesis processing (Farouqi et al. 2008a, 2008b).

2. CALCULATIONS AND RESULTS

The concept of an HEW arises from considerations of the newly born proto-neutron star in core-collapse supernovae. In this scenario, the late neutrinos interact with matter of the outermost neutron-star layers, leading to moderately neutron-rich ejecta with high entropies (see, e.g., Woosley et al. 1994; Takahashi et al. 1994; Qian & Woosley 1996; Hoffman et al. 1996, 1997; Freiburghaus et al. 1999; Thompson et al. 2001; Wanajo et al. 2006). In the present calculations, we follow the description of adiabatically expanding mass zones as previously utilized in Freiburghaus et al. (1999). The nucleosynthesis calculations up to charged-particle freezeout were performed with the latest Basel code (but without including neutrino–nucleon/nucleus interactions). The reaction rates were calculated by means of the statistical-model program NON-SMOKER (Rauscher & Thielemann 2000; T. Rauscher & F.-K. Thielemann 2007, private communication). The *r*-process network code now contains updated experimental and theoretical nuclear physics input on masses and β-decay properties, as outlined in Kratz et al. (2007b) and used in our earlier studies within the site-independent "waiting-point" approximation (Kratz et al. 2007a).

After charged-particle freezeout, the expanding, and eventually ejected, mass zones have different initial entropies ($S \sim T^3/\rho$ [k_b/baryon]), so that the overall explosion represents a superposition of entropies. The ratio of free neutrons to "seed" nuclei ($Y_n/Y_{\rm seed}$) is a function of entropy and, for high S, yields rapid neutron captures which can form the heaviest *r*-process nuclei. Furthermore, the ratio $Y_n/Y_{\rm seed}$ is correlated to the three main parameters of the HEW, i.e., the electron abundance ($Y_e = Z/A$), the entropy S, and the expansion velocity ($V_{\rm exp}$)

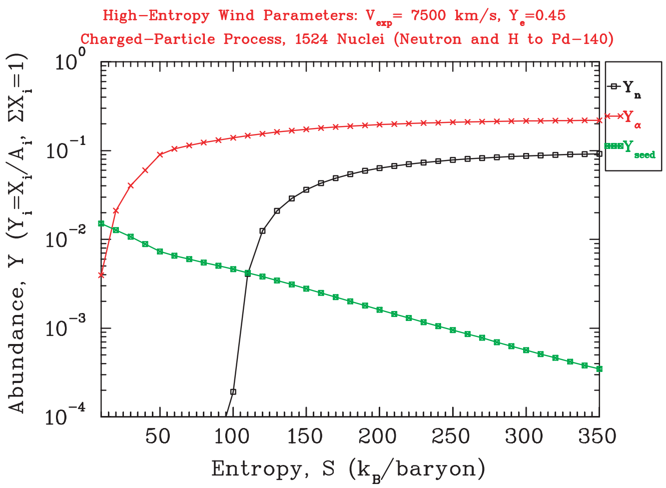

Figure 1. Abundance distributions ($Y_i = X_i/A_i$, $\Sigma X_i = 1$) of α-particles, heavy "seed" nuclei, and free neutrons as a function of entropy S at the freezeout of charged-particle reactions at $T_9 \simeq 3$.

(Hoffman et al. 1997; Freiburghaus et al. 1999). We determined the simple expression $Y_n/Y_{\rm seed} = 10^{-11} \times V_{\rm exp}\ (S/Y_e)^3$, valid in the parameter ranges $0.4 < Y_e < 0.495$, $1500 < V_{\rm exp} < 30{,}000$, and $1 < S < 350$. This ratio $Y_n/Y_{\rm seed}$ provides a measure of the strength of the r-process.

In the classical r-process approach, a range of neutron densities ($10^{20} < n_n < 10^{28}$) is necessary to reproduce the full distribution of the r-process "residuals" ($N_{r,\odot} = N_\odot - N_{s,\odot}$; Käppeler et al. 1989) up to the Th, U region (Kratz et al. 1993, 2007a, 2007b). In the HEW, at a given Y_e and $V_{\rm exp}$, the entropy (or the correlated $Y_n/Y_{\rm seed}$ ratio) will play this role. In the following, we will present selected nucleosynthesis results as a function of entropy (or $Y_n/Y_{\rm seed}$) for the (realistic and astrophysically interesting) choices $Y_e = 0.45$ and $V_{\rm exp} = 7500$ km s^{-1}—values taken from the much larger parameter space which was analyzed—and compare our HEW predictions to recent astronomical observations.

We first want to identify the abundance distributions that can be produced when utilizing the above parameter combination. In Figure 1, we show the abundance correlations of α-particles (Y_α), heavy "seed" nuclei ($Y_{\rm seed}$), and free neutrons (Y_n) as functions of entropy at the freezeout of charged-particle reactions. Over the entire entropy range displayed in this figure, most of the matter is locked into α-particles. In contrast to the smooth trend of Y_α, the abundance distributions of $Y_{\rm seed}$ and Y_n are strongly varying with entropy. For different values of Y_e and $V_{\rm exp}$, this behavior is shifted to lower/higher entropies. From the $Y_{\rm seed}$ and Y_n slopes it becomes evident that the HEW predicts—at least—two clearly different nucleosynthesis modes.

For the low entropy region ($1 \leqslant S \leqslant 110$), the concentration of free neutrons is negligible; hence, the nucleosynthesis in this region is definitely not a classical neutron-capture process but rather a charged-particle (α-) process. For higher entropies $Y_n/Y_{\rm seed}$ ratios increase smoothly, resulting for the region $110 \leqslant S \leqslant 150$ in a neutron-capture component that resembles a classical "*weak*" r-process. For even higher entropies ($150 < S < 300$), enough free neutrons are available to yield a classical "*main*" r-process (Hoffman et al. 1997; Meyer & Brown 1997; Freiburghaus et al. 1999; Pfeiffer et al. 2001). In Table 1, we show the contributions of certain entropy ranges to the production of elements (Z) in percent, under the assumption of equal-mass contributions per entropy interval for $1 < S < 300$.

Table 1
HEW Contributions to the Production of Selected Elements (Elemental Abundance, $Y(Z)$ in %) in the Fe to Ag Region for Different Entropy Ranges

Z	1	2	3	4
26	100.00	0.00	0.00	0.00
30	99.2	0.5	0.3	0.00
32	85.3	4.7	8.8	1.2
38	79.9	18.3	1.4	0.3
39	61.4	37.4	0.9	0.3
40	14.0	81.0	4.7	0.3
42	0.03	63.6	31.7	4.7
44	0.00	27.4	61.4	11.2
46	0.00	11.5	66.9	21.6
47	0.00	3.7	71.3	25.0

Notes. Column 1: S-range $1 < S < 50$, normal α-freezeout; Column 2: S range $50 < S < 110$, neutron-rich α-freezeout with βdn-recapture; Column 3: S range $110 < S < 150$, "*weak*" r-process; Column 4: S range $150 < S < 300$, "*main*" r-process. For discussion, see the text.

1. As can be seen from Table 1, in the lowest entropy range ($1 < S < 50$), we obtain a "normal" α-rich freezeout, mainly producing stable or near stable isotopes of elements in the region Fe to Sr (for further details, see Table 1 in Farouqi et al. 2008b). It should be noted that for varying choices of $Y_e = 0.45$–0.49, the classical "*s-only*" isotopes up to ^{96}Mo or even light "*p*-nuclei" up to ^{106}Cd can be produced.
2. In the next higher entropy range ($50 < S < 110$; Column 2 of Table 1), we again find that there are not enough free neutrons available to effect a neutron-capture process. Under these entropy conditions, however, the seed composition at freezeout is already shifted to the neutron-rich side of β-stability, including β-delayed neutron (βdn) precursor isotopes in the $80 < A < 100$ mass region (Pfeiffer et al. 2002). The resulting $Y_{\beta{\rm dn}}/Y_{\rm seed}$ conditions provide a low neutron density, S-like environment.
3. In the subsequent entropy range ($110 < S < 150$), the density of free neutrons ($1 \leqslant Y_n/Y_{\rm seed} \leqslant 10$) becomes high enough to start a "*weak*" r-process up to the rising wing of the $A \simeq 130$ $N_{r,\odot}$ peak. As shown in the third column of Table 1, under these conditions substantial concentrations of the elements Ru to Ag are produced.
4. For high entropies ($150 < S < 300$; now with $13 \leqslant Y_n/Y_{\rm seed} \leqslant 155$) the HEW predicts a very robust "*main*" r-process, starting with the $N = 82$ r-process progenitor isotopes of Tc to Rh at the onset of the $A \simeq 130$ peak and reaching up to the Th, U actinide region.

As a function of time, the HEW will eject matter with varying values of S, Y_e, and $V_{\rm exp}$. If one assumes that equal amounts of ejected material per entropy interval are contributing, the sum of the abundance contributions is weighted according to the resulting $Y_{\rm seed}$ as a function of entropy. Such a choice yields an SS-like isotopic abundance distribution ($N_{r,{\rm calc}}$) as displayed in Figure 2 in comparison to the standard r-process "residuals" $N_{r,\odot}$. The $N_{r,{\rm calc}}$ distribution represents a superposition of 15 equidistant S components in the range $160 \leqslant S \leqslant 287$. The lower limit of $S = 160$ has been chosen to restrict the calculations to representative "main" r-process conditions. Consequently, for this parameter choice no "best fit" to the light region below the $A \simeq 130$ peak is anticipated. The upper limit of $S = 287$ has been chosen to ensure that fission recycling remains negligible. We note that excellent overall agreement of

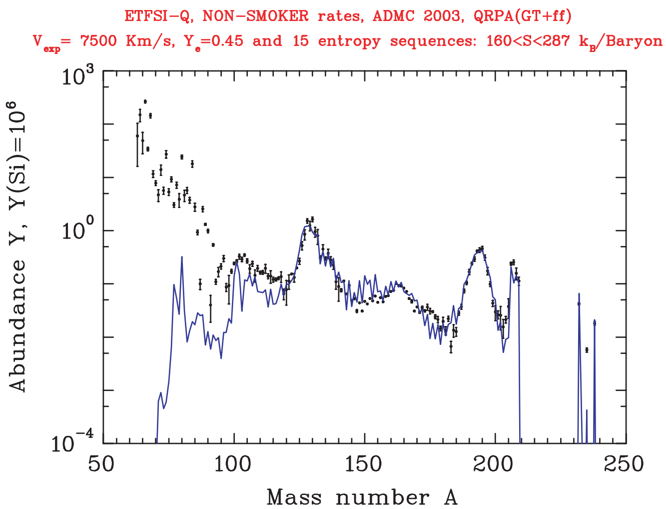

Figure 2. Comparison of the $N_{r,\odot}$ distribution (data points; Käppeler et al. 1989) with predicted isotopic abundances (solid line) from a weighted superposition of 15 HEW entropy components in the range $160 \leqslant S \leqslant 287$. For further details and discussion, see the text.

the $N_{r,\mathrm{calc}}$ distribution with the observed $N_{r,\odot}$ pattern is attained from the rising wing of the $A \simeq 130$ peak up to the Pb, Bi "spike."

It is also obvious that this superposition choice is not reproducing abundances from the Fe group to the rising wing of the $A \simeq 130$ peak. There have been a number of suggestions to fill in this region with a multiplicity of nucleosynthesis processes. As such elements are apparently already existing at low metallicities, but are not explainable by the traditional metallicity-dependent (secondary) *s*-process, a light element primary process (LEPP) was invoked by Travaglio et al. (2004), initially related to *s*-like neutron captures. Qian & Wasserburg (2007), following the initial argument of Hoffman et al. (1996, 1997), consider these elements to be primarily produced due to charged particle reactions (CPRs).

The HEW approach, with different choices of entropy superpositions for $S < 110$, is such a charged-particle process; for $110 < S < 150$ it also results in small neutron densities. We compare these predictions with recent astronomical observations of the abundances of elements between Cu and Ag, covering the range from "*r*-process-poor" stars such as HD 122563 up to "*r*-process-rich" stars such as CS 22892-052 (see, e.g., Figure 3 in Farouqi et al. 2008a). A crucial test would be that at least within a narrow S range, responsible for neighboring nuclei, the observed element ratios should be reproduced. Such a test avoids uncertainties in the choice of realistic entropy superpositions. When doing so for the Zn/Ge ratio, where observations (Cowan et al. 2005) show a factor beyond 100, our calculations—producing these nuclei for $S < 50$—would predict a ratio of 5. Thus, the present HEW conditions for Y_e values less than 0.5 disagree by a factor of 25. This disagreement can be avoided, when permitting proton-rich environments as discussed in the νp-process (Fröhlich et al. 2006; Pruet et al. 2006) during the very early phases of the neutrino wind, when even proton-rich conditions with $Y_e > 0.5$ are obtained. Such conditions are expected in every core-collapse supernova. The conclusion which emerges here is that although both environments involve charged-particle processes, the Y_e dependence plays a crucial role. An alternative is a strong primary *s*-process, occurring for massive stars at very low metallicities (Pignatari et al. 2008).

In Figure 3, we plot the LEPP abundance ratios, $\log(X/\mathrm{Zr})$, as a function of atomic number in the range $29 \leqslant Z \leqslant 50$ and compare the observational data with the predictions from two different nucleosynthesis approaches: (1) the present HEW superpositions with weights taken as in Table 1 and (2) the classical "waiting-point" model for a range of n_n conditions which fit best the low-mass region for *r*-process residuals (permitting also an extended seed composition below Fe). The observed $\log(X/\mathrm{Zr})$ pattern shows a decreasing slope with atomic number with a pronounced odd–even Z staggering. From Sr ($Z = 38$) upward, this trend is best reproduced by the HEW (with equal-mass superpositions in entropy S). In contrast, the high abundances observed for Cu ($Z = 29$) and Zn ($Z = 30$) obviously cannot be reproduced by any of the models, while proton-rich environments and the νp-process (Fröhlich et al. 2006; Pruet et al. 2006) show the option to do so. At the moment, we only can conclude that the major abundance fractions of the elements with $Z < 38$ are *not* produced together with the $Z \geqslant 38$ elements. Therefore, these light trans-Fe elements are also not produced under the same nucleosynthetic conditions as

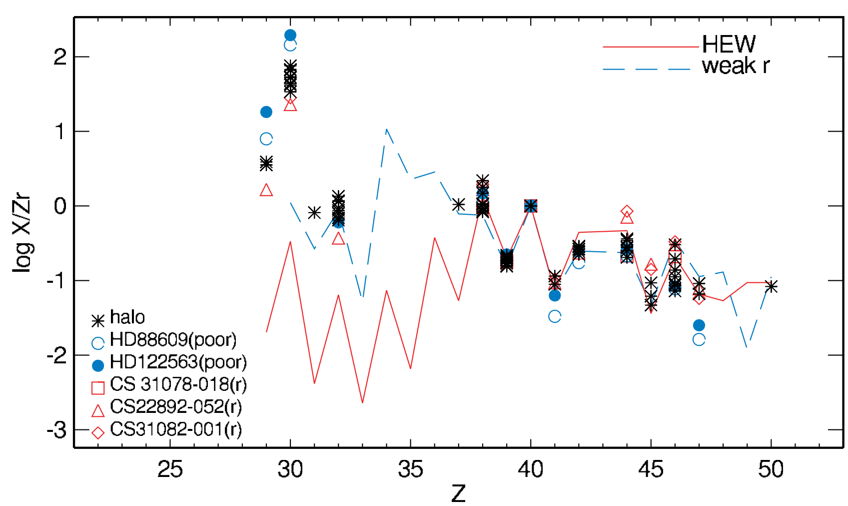

Figure 3. Elemental abundance ratios of $\log(X/\mathrm{Zr})$ as a function of atomic number Z. The observational data in the LEPP region between Cu ($Z = 29$) and Ag ($Z = 47$) for selected halo stars are given by different symbols explained in the lower-left corner of the figure. These data are compared with predictions from two different nucleosynthesis approaches: (1) the present HEW model (solid line); (2) the classical "waiting-point" model for a "weak" *r*-process with a low n_n-range solar-like Si–Cr seed composition (dashed line). For discussion, see the text.

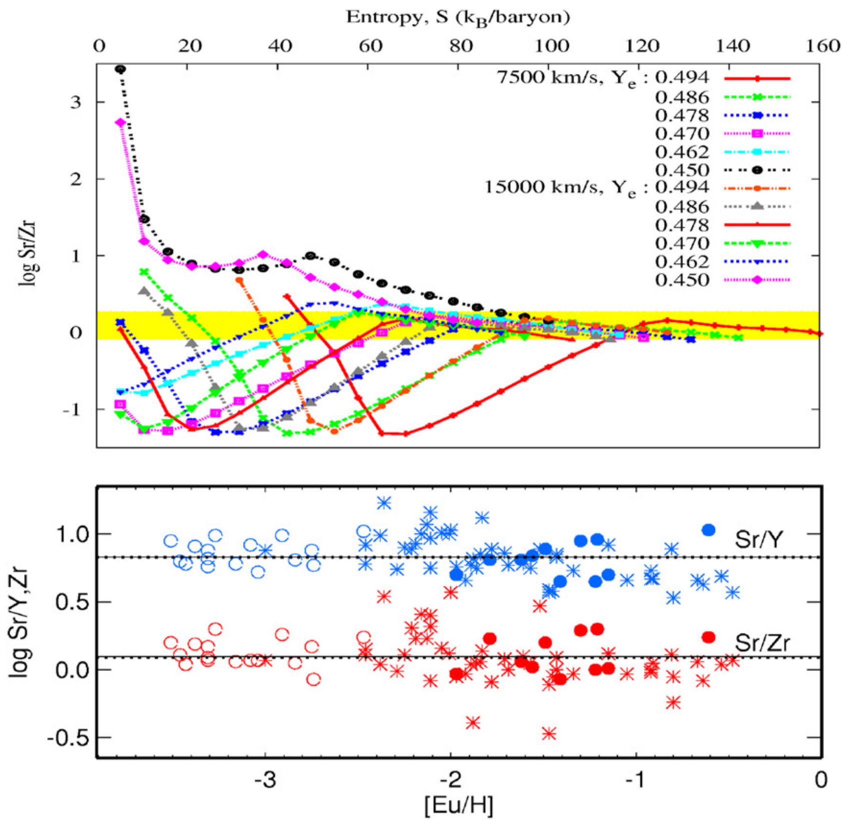

Figure 4. Top panel: Sr/Zr ratio as predicted from HEW calculations for different values of Y_e as a function of entropy S. The observed value is shown by gray color band. Bottom panels: elemental abundance ratios of log(Sr/Y, Zr) as a function of r-process enrichment [Eu/H] for halo stars in our Galaxy. The observational data with their mean values shown as solid lines are compared to the abundance predictions of our HEW model (dotted lines, partly indistinguishable from the solid lines) for the low-S range ($1 \leqslant S \leqslant 110$) of the α-component. For discussion and the sources of observational data, see the text.

Eu, and should be uncorrelated with the "main" r-process. This result is, indeed, confirmed for Ge abundances recently obtained from *Hubble Space Telescope* observations (Cowan et al. 2005).

We now consider the three LEPP neighbors Sr, Y, and Zr, for which two independent large data sets from (1) Barklem et al. (2005) and Mashonkina et al. (2007) (B&M set) and (2) from François et al. (2007) exist. These data sets agree very well in showing that the abundances of Sr, Y, and Zr, viewed as separate elements, are not tightly (but partially) correlated with the (almost pure) "main" r-process element Eu. The elemental abundance ratios of log(Sr/Y/Zr) from Galactic halo stars, e.g. as a function of metallicity [Fe/H], r-process enrichment [Eu/H] or LEPP enrichment [Sr/H] have been shown to exhibit a robust, constant pattern (see, e.g., Travaglio et al. 2004; Qian & Wasserburg 2007; Mashonkina et al. 2007; François et al. 2007). Early studies (Hoffman et al. 1996) seemed to indicate a strong Y_e dependence for the light trans-Fe elements (for entropies $S < 50$). We have done calculations to predict the elemental ratios in this mass region for a variety of entropies. What is noticed is that for the higher entropies which contribute to this mass range ($60 < S < 110$, see Table 1) the elemental ratios are converging to the observed ones, as indicated for Sr/Zr in the top frame of Figure 4, but has also been tested for Sr/Y and Y/Zr. For lower entropies, also contributing to these elements, we see for each Y_e a variation as a function of entropy, leading on average also to values close to the observed ones. Thus, when integrated over the relevant S conditions, these abundances seem to be independent of Y_e and reproduce the observed abundance ratios very well. This indicates that in a superposition over entropies the Sr/Y/Zr elements can be co-produced with the observed abundance ratios (see in Figure 4—lower two panels—(Sr/Y, Zr) as a function of "r-process enrichment" in the range $-3.5 \leqslant$ [Eu/H] $\leqslant -0.5$ from the B&M data set and also data from Cowan et al. (2002); François et al. (2007); Hill et al. (2002); Honda et al. (2004, 2006, 2007); Ivans et al. (2006); Lai et al. (2008); Sneden et al. (2003), but also Figure 3 for $Z = 38$, 39 and 40).

The mean values of the observed abundance ratios (log(Sr/Y) $= 0.83 \pm 0.15$ and log(Sr/Zr) $= 0.09 \pm 0.18$) are very well reproduced (log(Sr/Y) $= 0.83$ and log(Sr/Zr) $=$ 0.13) by the low-S ($S < 110$) charged-particle (α-) component of the HEW, dominating that mass range. When comparing the observed data set to HEW predictions, restricted to higher entropies ($110 \leqslant S \leqslant 280$) which lead to a neutron-capture r-process, the resulting ratios log(Sr/Y) $= 0.99$ and log(Sr/Zr) $= -1.38$ indicate that this nucleosynthesis mode is unimportant for that mass range. This is consistent with the fact that the element correlations [Zr/Fe] versus [Eu/Fe] (in analogy to Figure 6 in Cowan et al. (2005)) clearly show—now for an ensemble of 83 halo stars in the range $-0.7 \leqslant$ [Eu/Fe] $\leqslant 1.7$—that the above LEPP elements are not tightly correlated with the r-process indicator Eu.

We also want to call attention to the recent accumulation of abundance data on the two light platinum-group elements (PGEs) Ru ($Z = 44$) and Pd ($Z = 46$) for the extremes of "r-poor" stars (such as HD 122563; Honda et al. 2006) and "r-rich" stars (such as CS 22892-052; Sneden et al. 2003). Table 1 indicates that both elements can be co-produced in substantial fractions by the charged-particle component (i.e., α-freezeout, together with Sr–Zr) and the neutron-capture (r-)

component together with the nucleosynthesis of $A = 130$ peak elements Sn–Te. In halo stars and r-rich but α-component-poor stars, the mean values of the observations are log(Pd/Sr) = −0.95 and log(Pd/Eu) = 0.81. For r-poor but α-component-rich stars the observed abundance ratios are log(Pd/Sr) = −1.16 and log(Pd/Eu) = +1.5. This indicates that for the halo and r-rich stars the dominant r-component of Pd correlates with Eu, whereas for the r-poor stars the α-component of Pd dominates and is correlated with Sr.

The question remains whether the observed Ru/Pd ratios can also be reproduced by our HEW superpositions. Figure 3 indicates a good average trend of the canonical equal-mass superposition per entropy for $Z = 44$ and 46. Observations in low-metallicity stars are scarce, log(Ru/Pd) seems to cluster around 0.27 ± 0.05 for normal halo stars (from determinations in this study and in Ivans et al. 2006) and around 0.39 for two r-rich stars (Hill et al. 2002; Sneden et al. 2003). On the other hand, two stars which show features of the weak r-process are reported to have log(Ru/Pd) = 0.47 (Honda et al. 2007, 2006), although it is worth noting that the Pd abundance in these stars was derived from the only Pd I 3404 line. If we analyze the predictions obtained from entropy components contributing to the mass region of interest, we find a downshift in log(Ru/Pd) by about 0.2 between the entropy regions $100 < S < 150$ and $150 < S < 200$, i.e. lower Ru/Pd ratios when changing from weak to main r-process sources, which is consistent with observations. However, the absolute value is Y_e dependent (with a ratio close to 0.5 rather than 0.39 for $Y_e = 0.45$ and high entropies). Thus, if the nuclear input is sufficiently reliable, future improvements in models and observations could provide further insight into the necessary features of the astrophysical site (including Y_e requirements).

3. SUMMARY AND CONCLUSIONS

We have performed large-scale dynamical network calculations in the context of an adiabatically expanding HEW as expected in core-collapse SNe II. We find that the correlated parameters that act to determine the strength of the astrophysical r-process, reflected in the ratio $Y_n/Y_{\mathrm{seed}} = 10^{-11} \times V_{\mathrm{exp}}\ (S/Y_e)^3$, show a surprisingly robust picture for the production of heavy elements beyond Fe. Our results suggest astrophysical conditions for the HEW scenario which reproduce the solar r-abundances quite satisfactorily without invoking more exotic nucleosynthesis scenarios or nuclear physics assumptions.

We also tested how important the HEW scenario is for the light-Z region between Cu and Rb. Neither the Cu/Zn/Ge abundance ratios nor the absolute yields observed in halo stars can be reproduced in an entropy superposition with $Y_e < 0.5$, which clearly indicates another nucleosynthesis origin. For Sr to about Mo the dominating production is related to low entropies ($S \leqslant 110$), where the charged-particle (α-rich) freezeout results in entropy-dependent "seed" nuclei smoothly shifting from β-stability to the neutron-rich side. However, the entropy conditions relevant for the respective elements lead to element ratios, e.g. Sr/Y/Zr or Ru/Pd, which seem consistent with astronomical observations. Rapid neutron-capture nucleosynthesis only sets in at higher entropies, where the range $110 \leqslant S \leqslant 150$ produces elements up to the rising wing of the $A \simeq 130$ $N_{r,\odot}$ peak under "weak" r-process conditions, whereas for $150 \leqslant S \leqslant 300$ a robust "main" r-process between $A \simeq 120$ and the actinide region occurs. The HEW with an entropy superposition of equal-mass ejecta per entropy interval is able to reproduce the overall $N_{r,\odot}$ "residuals" beyond Sn, as well as all major recent observations from metal-poor halo stars.

Thus, all heavy elements beyond Sr and their classical r-(residual) abundances can potentially be reproduced in entropy superpositions, which for $S \geqslant 60$ seem essentially independent of Y_e (in the range $0.45 \leqslant Y_e \leqslant 0.49$). In the lower entropy range results are Y_e dependent, and in addition to r-nuclei also classical "s-only" isotopes as well as p-nuclei can be produced in the range ^{54}Fe up to ^{106}Cd. These results provide the means to substantially revise the abundance estimates of different primary nucleosynthesis processes for elements in the historical "weak-s"/"weak-r" process region and to quantify their correlation with the "main" r-process.

To obtain more quantitative answers to questions concerning the astrophysical site of the compositions of the LEPP elements between Sr ($Z = 38$) and Cd ($Z = 48$), as well as all of the n-capture elements, will require more and higher-quality observational data and also more realistic values of entropy superpositions derived from hydrodynamical models.

We thank R. Gallino for helpful discussions. Partial financial support for this research was provided by the Deutsche Forschungsgemeinschaft (DFG), the Helmholtz Gemeinschaft, the NSF, the DOE as well as the Swiss NSF.

REFERENCES

Argast, D., et al. 2004, A&A, 416, 997
Barklem, P. S., et al. 2005, A&A, 439, 129
Burbidge, E. M., et al. 1957, Rev. Mod. Phys., 29, 547
Cameron, A. G. W. 1957, PASP, 69, 201
Cowan, J. J., & Sneden, C. 2006, Nature, 440, 1151
Cowan, J. J., et al. 1991, Phys. Rep., 208, 267
Cowan, J. J., et al. 2002, ApJ, 572, 861
Cowan, J. J., et al. 2005, ApJ, 627, 238
Farouqi, K., et al. 2008a, AIP Conf. Proc., 990, 309
Farouqi, K., et al. 2008b, AIP Conf. Proc., 1001, 245
François, P., et al. 2007, A&A, 476, 935
Freiburghaus, C., et al. 1999, ApJ, 516, 381
Fröhlich, C., et al. 2006, Phys. Rev. Lett., 96, 142502
Hill, V., et al. 2002, A&A, 387, 560
Hoffman, R. D., et al. 1996, ApJ, 460, 478
Hoffman, R. D., et al. 1997, ApJ, 482, 951
Honda, S., et al. 2004, ApJ, 607, 474
Honda, S., et al. 2006, ApJ, 643, 1180
Honda, S., et al. 2007, ApJ, 666, 1189
Ivans, I., et al. 2006, ApJ, 645, 613
Käppeler, F., et al. 1989, Rep. Prog. Phys., 52, 945
Kratz, K.-L., et al. 1993, ApJ, 403, 216
Kratz, K.-L., et al. 2007a, ApJ, 662, 39
Kratz, K.-L., et al. 2007b, Prog. Part. Nucl. Phys., 59, 147
Lai, D. K., et al. 2008, ApJ, 681, 1524
Mashonkina, L. I., et al. 2007, Astron. Rep., 51, 903
Meyer, B. S., & Brown, J. S. 1997, ApJS, 112, 119
Pfeiffer, B., et al. 2001, Nucl. Phys., A693, 282
Pfeiffer, B., et al. 2002, Prog. Nucl. Energy, 41, 39
Pignatari, et al. 2008, ApJ, 687, L95
Pruet, J., et al. 2006, ApJ, 644, 1028
Qian, Y.-Z., & Wasserburg, G. J. 2007, Phys. Rep., 442, 237
Qian, Y.-Z., & Woosley, S. E. 1996, ApJ, 471, 331
Rauscher, T., & Thielemann, F.-K. 2000, ADNDT, 75, 1
Sneden, C., & Cowan, J. J. 2003, Science, 299, 70
Sneden, C., et al. 2003, ApJ, 591, 936
Takahashi, K., et al. 1994, A&A, 286, 857
Thompson, T. A., et al. 2001, ApJ, 562, 887
Travaglio, C., et al. 2004, ApJ, 601, 864
Wanajo, S., et al. 2006, ApJ, 636, 842
Woosley, S. E., et al. 1994, ApJ, 433, 229